JOURNAL OF BIOMEDICAL OPTICS 3(3), 267–280 (JULY 1998)

BAND ANALYSIS OF HYDRATED HUMAN SKIN STRATUM CORNEUM ATTENUATED TOTAL REFLECTANCE FOURIER TRANSFORM INFRARED SPECTRA *IN VIVO*

Gerald W. Lucassen,[†] Gerard N. A. van Veen,[†] and Jan A. J. Jansen[‡]
[†]Personal Care Institute, Philips Research; [‡]Materials Analysis, Philips Centre for Manufacturing Technology, Prof. Holstlaan 4, Eindhoven, The Netherlands

(Paper JBO-171 received Sep. 27, 1997; revised manuscript received Feb. 20, 1998; accepted for publication Feb. 24, 1998.)

ABSTRACT

Water content is an important factor for skin condition. The determination of the hydration state of the skin is necessary to obtain basic knowledge about the penetration and loss of water in the skin stratum corneum. Attenuated total reflectance Fourier transform infrared (ATR-FTIR) spectroscopy is used to measure hydration of the stratum corneum. In this study we apply direct band fitting of the water bending, combination, and OH stretch bands over the 4000–650 cm^{-1} wave number range. Measurements are performed on the volar aspect of the forearm using a Nicolet 800 FTIR spectrometer equipped with an ATR unit with a ZnSe crystal. Hydration of the skin is obtained by occlusion keeping the forearm pressed onto the crystal. Spectra are recorded before and after occlusion up to 30 min. The spectra are fitted with a nonlinear least-squares algorithm with Gaussian bands. Separate band fits of water, normal stratum corneum, and occluded hydrated stratum corneum spectra are obtained yielding band parameters of the individual water contributions in the bending mode at 1640 cm^{-1}, the combination band at 2125 cm^{-1}, and the OH stretches in the hydrated skin stratum corneum spectra. A scaling factor representing the contribution of the water spectrum into the skin stratum corneum spectrum is determined during the occlusion process. In comparison to the dependence of the infrared absorbance ratio in time used by Potts, our scaling factor shows a more distinct transition from enhanced signal due to increased contact area to extra signal due to water content at maximum contact area. Band fit analysis of hydrated skin stratum corneum ATR-FTIR spectra offers the possibility for quantitative determination of individual water band parameters.
[S1083-3668(98)01203-9]

Keywords stratum corneum; water; hydration; fit analysis; moisturing factor; absorbance ratio; penetration depth.

1 INTRODUCTION

Noninvasive skin hydration measurements are of increasing importance in dermatology, pharmacology, cosmetics, and the medical sciences for the monitoring of the skin condition and to attain understanding of the skin hydration. Various techniques exist to measure water in skin, each with its own sensitivity, resolution, and depth range. For reviews on these techniques see Refs. 1 and 2.

Hydration of the skin stratum corneum (SC) has been studied in the 1960's and 1970's by Puttnam et al.,[3] and Hansen and Yellin[4,5] using attenuated total reflectance (ATR), nuclear magnetic resonance, and infrared (IR) spectroscopy. From *in vitro* studies they found three types of water in the SC with different hydrogen bonding strengths, mobilities and sorption, and desorption kinetics. Below 10% (w/w) hydration (water weight to dry weight SC), water is tightly bound to the polar sites of the SC keratin proteins (primary hydration). At water concentrations from 10% to 40% less tightly bound water is found, probably hydrogen bonded to primary water (secondary hydration). At higher concentrations in the SC, water behaves more like bulk liquid water. Recent near-infrared *in vivo* spectroscopic studies by Martin[6] showed evidence of the three types of water mentioned above as well. Besides these hydration states, Martin introduces water associated to the lipid phase within the SC, which may be responsible for the evaporative flux across the SC.

For the period up to 1985, a summary of studies on the effect of humidity on both strength and number of water binding sites in the SC can be found in Potts.[1] A number of water peaks in the

Address all correspondence to Dr. Ir. Gerald W. Lucassen, Personal Care Institute, Philips Research, Prof. Holstlaan 4, (WB32), 5656AA Eindhoven, The Netherlands; Tel.: +31-40-2743648; Fax: +31-40-2744288; E-mail: lucassen@natlab.research.philips.com

1083-3668/98/$10.00

infrared spectra is attributed to different SC water binding sites. From combined *in vitro* and *in vivo* experiments using attenuated total reflectance Fourier transform infrared spectroscopy (ATR-FTIR) Potts et al.[7] quantitatively determined the water content in the stratum corneum.

The same technique was used by Bommannan et al.[8] to study the barrier function of the SC *in vivo*. Boddé et al.[9] and Wichrowski et al.[10] studied hydration of the skin applying cosmetic moisturizers using ATR-FTIR.

In this paper we apply ATR-FTIR spectroscopy to investigate the vibrational characteristics of *in vivo* skin SC on hydration. ATR-FTIR is a suitable noninvasive technique to determine skin hydration *in vivo*, not only because water absorbs strongly in the infrared, but also because the spectra of water and skin constituents can (in principle) be uniquely identified. The measuring depth of ATR-FTIR in the skin is typically a few microns over the wave number ($\nu = 1/\lambda$) window 4000–650 cm^{-1}. This means that ATR-FTIR enables us to monitor changes in water content of the most outer SC layers directly. This is important as it also gives information about the barrier function of the skin. Gloor et al.[11] obtained the water content from the amide I and amide II band ratio, or ''moisturing factor'' (MF).

It was found that this ratio could be used to measure the water content qualitatively. However, as Potts pointed out[7] the amide I and amide II band change in intensity in different ways with increasing water content. The method used by Potts[7] focuses on the combination band at 2100 cm^{-1}. The area under the curve above the line connecting the spectral intensity at 1900 and 2300 cm^{-1} is considered as a measure of the water content, whereas the area under this base line is considered as a measure of contact area. The ratio of these two areas is called the infrared absorption ratio. From a comparison of infrared absorption ratios obtained *in vivo* with those measured *in vitro*, quantitative information on hydration is obtained.

In the Potts method a problem arises at low water content. The shape of the 2100 cm^{-1} band is obscured due to the influence of the high intensity band at 1640 cm^{-1} and the broad higher wave number bands, which affects the analysis. Also, amplitude and integrated band intensity of the OH stretch region around 3300 cm^{-1} has been used as a measure of stratum corneum hydration.[10] This broad band contains several types of OH stretch vibration bands.

The three methods mentioned above are of practical use; they can be applied directly using the measured absorbances. However, problems arise when taking absorbance maxima that do not correspond to the actual absorbances at the real band frequencies as, for example, is the case with the moisturing factor method. Also, the band shape changes around the 2100 cm^{-1} combination band at low water concentrations cause a problem in determining the actual water content. When using absorbances or integrated intensity of the OH stretch band region, the situation is complex, since it also contains a contribution from a NH-stretch band, that varies with water content. We have tried to circumvent these problems by using the spectral band information known from literature and using direct band fit analysis of the spectra. This has the advantage of using the entire spectral range, covering the three regions of interest by the methods mentioned above. Furthermore, the actual water band parameters (frequency, amplitude, and bandwidth) directly relate to the water content in the skin SC.

The water band structures have been intensively studied by Draegert et al.,[12] Williams,[13] and recently by Marechal[14–16] using infrared spectroscopy, and by Scherer et al.[17,18] and Moskovits et al.[19] using Raman spectroscopy. From the comparison of polarized Raman spectra, infrared spectra on H_2O, D_2O, and HDO mixtures and normal mode calculations by Curnutte et al.[20–22] many of the observed bands could be assigned. Still, the details of water at the molecular level are not completely understood. The high density of hydrogen bonds and the quasitetragonal symmetry of water makes such a description very complex.[14–16,23,24] Recently, Barry et al.[25] and Edwards et al.[26] have measured Fourier transform Raman and infrared spectra of *in vitro* human skin and listed assignments of the spectral bands.

In this paper information on assignments of the water bands known from IR and Raman studies is combined with band fits on ATR-FTIR spectra of hydrated skin stratum corneum *in vivo*. The purpose is to use spectral fit analysis to determine the contribution of water bands in the skin SC spectrum, covering the above-mentioned three regions of interest. In this paper two fit methods are used. In the first method all skin and water bands are considered having free parameters, whereas in the second method the liquid water spectrum as separately measured is fitted into the skin SC spectrum taking a scaling factor as a free parameter, thereby keeping the individual water band amplitude ratios constant. Band frequencies known from literature are given fixed values in the fits, all other unknowns were free parameters. It will be shown that these fit methods yield detailed information on skin SC and water band contributions enabling determination of water content. The results are compared with the MF and IR absorbance ratio methods used by Gloor and Potts, respectively.

2 MATERIAL AND METHODS

2.1 EXPERIMENT

The ATR-FTIR spectra are recorded on a dry air flushed Nicolet-800 Fourier transform spectrometer

equipped with a liquid N_2 cooled mercury cadmium telluride (MCT) detector and a ''high-top'' model ATR with a ZnSe ($n=2.42$) or Ge ($n=4.0$) crystal of rectangular shape (10 mm×80 mm) with 45° entrance and exit facets. The shape of the crystal limits the number of reflections inside the crystal to 10. Typically, the ATR-FTIR spectrum is obtained by the Fourier transform of 64 coadded interferograms, where Happ–Genzel apodization is used. At a resolution of 8 cm^{-1} the acquisition time for 64 scans is 20 s. Spectra are recorded in the 4000–650 cm^{-1} range, which is the transparent region of the ZnSe crystal for the IR beam. Files are converted to absorbance and stored to disk for further processing and displaying. Water spectra are recorded from distilled water using a Ge ($n=4.0$) crystal trough instead of the ZnSe crystal to limit penetration of the evanescent wave and prevent signal saturation in the higher wave number range. Skin SC spectra are recorded on the volar aspect of the authors' forearms by a slight pressure on the ZnSe crystal. Before the measurements, the skin is cleaned using a 1% solution of sodium lauryl sulphate in water, rinsing with water, and drying with paper towels. This cleaning removes possible dirt and sebum on the skin surface that could possibly disturb the spectra. Hydration of the skin is obtained by occlusion keeping the forearm on the crystal for about 30 min while recording a spectrum each minute. This has the advantage of measuring the same position of the skin SC of the arm each time.

2.2 SPECTRAL ANALYSIS AND BAND FITTING

Spectral analysis is performed by band fitting based on a nonlinear least-squares search using Gaussian band intensity shapes of the form $I_i(x)=A_i \times \exp\{-[(x-\Omega_i)/\Gamma_i]^2\}$ where I represents the infrared absorbance, x the running wave number variable and Ω_i the frequency, Γ_i the width, and A_i the amplitude of the ith band. The program enables simultaneous fitting of a chosen number of bands where band frequency, width, and amplitude can be selected to be ''fixed'' or ''free running'' parameters. Band frequencies known from literature are fixed. This means that we neglect possible frequency changes induced by hydration. All other parameters are free running parameters. Separate fits of normal skin SC spectra and hydrated skin SC spectra, and of the pure water spectrum are performed. We use two methods to fit normal and hydrated skin SC spectra. In the first method the widths and amplitudes of the skin SC bands including the individual water bands are treated as free parameters.

The water content is obtained from the amplitudes in the three water band regions of interest. In the second method we are interested to see whether the water content can be determined by fitting a scaling parameter S which varies the amplitude of the water spectrum over the entire range, keeping the ratios of amplitudes of all individual water bands constant:

$$I(x)=I_{SC}(x)+S^{*}I_{H_2O}(x). \quad (1)$$

Good fits are obtained by interactive control of parameters looking at least squares values of the fits.

3 RESULTS

3.1 NORMAL SKIN SC SPECTRUM

An ATR-FTIR spectrum of untreated *in vivo* skin SC is displayed in Figure 1(a). Detailed assignments are given in Figures 1(b) and 1(c). Table 1 gives the band assignments as known from the literature.[17,18,25] A number of bands can clearly be distinguished in the FTIR spectrum. Dominant bands are due to the amides at 1650 cm^{-1} (amide I, C=O stretching in O=C–N–H) and 1545 cm^{-1} (amide II, N–H bending in O=C–N–H). The amide parts of the spectrum carry structural information on the backbone of proteins (keratins) and lipids (ceramides), which make up the so-called ''mortar and brick'' in SC. Human stratum corneum consists for 75%–80% by weight of keratin proteins (α-keratin 70%, β-keratin 10%) and 5%–15% by weight of lipids (ceramides, free fatty acids, cholesterol, cholesterol sulfate, etc.). From this it can be inferred that the protein:lipid contribution to the amide amplitudes is about 8:1.

A specific band is the 1740 cm^{-1} band, the C=O stretching band of lipid ester carbonyl, indicative of the presence of sebum in the SC. In spectra taken on the forehead, cheek, or neck, two peaks with different amplitudes belonging to the two carbonyl groups in lipid ester appear at 1708 and 1740 cm^{-1} (spectra not shown). Generally the bending modes have smaller frequencies as compared to most stretching frequencies. For example, the C–H bending of lipids is found at 1451 cm^{-1}, and C–H stretches in asymmetric and symmetric CH_2 and CH_3 modes of lipids at 2851 and 2919 cm^{-1}, respectively. The broad band around 3300 cm^{-1} contains OH stretches and a NH stretch. In the normal SC spectrum water bands are present as well. These water bands will be described in more detail below.

3.2 ATR-FTIR SPECTRUM OF WATER

The measured ATR-FTIR spectrum (solid line) and fit (dashed line) of water at room temperature are shown in Figure 2. Table 2 overviews the water band assignments extracted from literature and also gives the fit parameters.

3.2.1 Bending Mode and Low Wave Number Region

At the low wave number edge of the spectrum the wing of the ''libration'' band ν_L is seen, associated

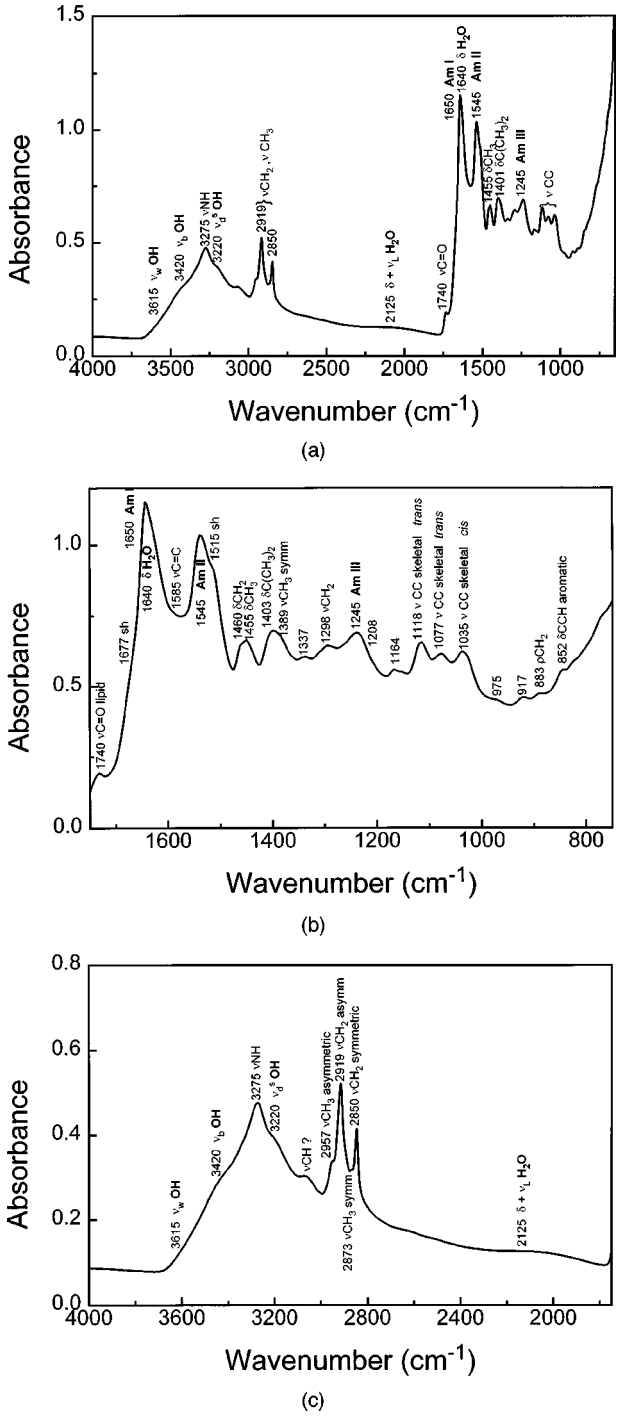

Fig. 1 (a) Measured ATR-FTIR spectrum of human skin stratum corneum on the volar aspect of the forearm *in vivo*, (b) details of the 750–1750 cm^{-1} spectral range, (c) details of the 1750–4000 cm^{-1} spectral range. Assignments are indicated in the figure (see also Table 1).

with vibrations around the three rotational axes of the water molecule. The sharp band at 1640 cm^{-1} (of the liquid water) corresponds with the δ (H_2O) bending mode ν_2 of the isolated water molecule centered at 1595 cm^{-1} in vapor. This band is on top of some broadbands on either side. Around 2125 cm^{-1} a weak band is seen that has been assigned to the $\delta+\nu_L$ combination band of the bending mode at 1640 cm^{-1} and the libration band ν_L. Similarly, the $\delta-\nu_L$ combination band is expected at the low wave number side of the 1640 cm^{-1} band around 1155 cm^{-1}. However, the latter band is not a distinctly visible feature because it is obscured by a broad feature between the libration band and the bending mode band. These combinations point to a libration band frequency ν_L at 485 cm^{-1}. From IR measurements by Draegert et al.[12] only an absorption maximum at 685 ± 15 cm^{-1} was found which was assigned to "hindered rotation" mode ν_R. Also a translational mode ν_T at 170 ± 15 cm^{-1} could be identified. Williams[13] proposed that the 2125 cm^{-1} band would be a combination of $\nu_2+\nu_R-\nu_T$ which is a transition starting from the first excited translational state. However, the difference $\nu_R-\nu_T=515$ cm^{-1} can only be matched to the 485 cm^{-1} if the frequency accuracy ranges of the ν_R and ν_T bands are coadded.

3.2.2 OH Stretch Region

The literature on the assignments of the broad OH stretch bands of water is scarce. On the basis of polarized Raman spectra Scherer et al.,[17,18] propose a model of water that classifies two species of hydrogen bonded water complexes: one symmetric and one asymmetric water complex. In both complexes the central water molecule is bonded to other water molecules by bonds between two hydrogens of two other water molecules to the oxygen side of the central water molecule. In such complexes the hydrogen bonds between the molecules can be loose or tight. The symmetric complex has two strong H bonds, having a symmetric OH stretch ν_d^s at 3220 cm^{-1} and an asymmetric OH stretch ν_d^{as} at 3440 cm^{-1}.[17,18] Both are IR active, the first is Raman active in the anisotropic Raman spectrum, the latter does not show up in the isotropic Raman spectrum. The asymmetric water complex has one strong H bonded OH stretch ν_b at 3425 cm^{-1} and one weak H bonded OH stretch ν_w at 3615 cm^{-1}. Also Fermi resonance of the bending overtone $2\nu_2$ with the ν_d^s and ν_b OH stretches contributes to the broad OH band region. In Raman spectra it has been shown that this Fermi resonance is necessary to explain the band shape of the broad OH stretch bands.[17,18] In the IR spectra this effect is less pronounced and we were able to obtain good fits without inclusion of the Fermi resonance. An important conclusion from the work by Scherer et al.[17,18] is that a considerable part of the water molecules is suggested to have one hydrogen strongly bonded while the other hydrogen is comparatively free at room temperature.

3.3 MONITORING SKIN HYDRATION

Hydration of the skin through occlusion can be achieved by keeping the forearm pressed against

Table 1 FTIR frequencies (cm^{-1}) and assignments of vibrational bands of human stratum corneum according to Barry et al. (Ref. 25)[a] and Scherer et al. (Refs. 17 and 18)[b] and frequencies found in our study (Figure 1). v=very; s=strong; m=medium; w=weak; sh=shoulder; br=broad; δ=deformation; ν=stretch; ρ=rock.

Frequency (cm^{-1}) Barry,[a] Scherer[b]	Frequency (cm^{-1}) This study		Assignment
3615[b] vw	3615	vw	ν_w(OH) weak bond of H_2O
3420[b] ms	3420	ms	ν_b(OH) strong bond of H_2O
3287[a] vs,br	⋯		ν(OH) of H_2O
3300[a]	3275	ms	ν(NH)
3220[b] ms	3220	ms	ν_d^s(OH) symmetric of H_2O
3070[a] w	⋯		1st overtone amide II at 1548 cm^{-1}
⋯	3050	w	ν(CH)?
2957[a] w	2957	w	$\nu(CH_3)$ asymmetric
2919[a] vs	2919	vs	$\nu(CH_2)$ asymmetric
2873[a] w	2873	w	$\nu(CH_3)$ symmetric
2851[a] s	2851	s	$\nu(CH_2)$ symmetric
2125[b] m	2125	m	$\delta + \nu_L(H_2O)$ combination
1743[a] w	1740	w	ν(C═O) lipid
⋯	1677	sh	shoulder
1656[a] vs	⋯		ν(C═O) amide I disordered
1650[a] vs	1650	vs	ν(C═O) amide I α-helix
⋯	1640	vs	$\delta(H_2O)$ bending
⋯	1585	w	ν(C═C) olefinic?
1548[a] vs	1545	s	δ(NH) and ν(CN) amide II
⋯	1520	m	water combination band
1515[a] w,sh	1515	m,sh	shoulder
1460[a] vw	1460	m,sh	$\delta(CH_2)$
1451[a] vw	1455	m	$\delta(CH_3)$ asymmetric
1440[a] vw	⋯		$\delta(CH_2)$ scissoring
1401[a] w	1403	m	$\delta[C(CH_3)_2]$ symmetric
1389[a] vw	1389	sh	$\delta(CH_3)$ symmetric
1366[a] vw	⋯		$\delta[C(CH_3)_2]$ symmetric
⋯	1337	vw	?
1298[a] w	1298	w	$\delta(CH_2)$
1247[a] w	1245	m	$\delta(CH_2)$ wagging; ν(CN) amide III disordered
⋯	1164	w	ν (CC), δ(COH)
⋯	1118	m	ν (CC) skeletal *trans* conformation
1076[a] w	1077	m	ν (CC) skeletal *trans* conformation

Table 1 (*Continued*).

Frequency (cm^{-1}) Barry,[a] Scherer[b]	Frequency (cm^{-1}) This study	Assignment
⋯	1035 m	ν(CC) skeletal *cis* conformation
⋯	975 vw	?
⋯	917 vw	?
⋯	883 vw	$\rho(CH_2)$
⋯	852 vw	δ(CCH) aromatic

the crystal. A clear increase in the IR signal is observed during the occlusion period of 30 min while recording a spectrum every minute, see Figure 3. The spectra are not scaled. By keeping the arm on the crystal, water cannot evaporate and accumulates in the skin SC. The observed signal increase in most parts of the spectra is due to (a) increased contact area between skin and crystal, and (b) an increase of water content in the skin SC.

Upon hydration, the keratinocytes will be plastified, which makes it easier to conform the uppermost keratine cells to the crystal surface. Once this contact area is at a maximum, further signal increase is due to an increase of water content in the SC. One can clearly see the influence of the water bands in the skin stratum corneum spectrum. Examples of spectral fits to the fully hydrated SC spectrum of Figure 3 are presented in Figure 4(a) for fit method 1 and Figure 4(b) for fit method 2. Parameters of the fits are listed in Tables 3(a) and 3(b). Following Scherer we have fitted the broad OH band of water using the symmetric stretch ν_d^s(OH) at 3220 cm^{-1}, the strong bond ν_b(OH) stretch at 3422 cm^{-1}, and the weak bond ν_w(OH) stretch at 3615 cm^{-1}. The ν_d^{as}(OH) at 3440 cm^{-1} has been merged with the strong bond ν_b(OH) stretch at 3420 cm^{-1} because these bands are close together.

From the hydrated spectra and fits we have plotted in Figure 5 the moisturing factor MF as used by Gloor et al.[11] obtained from the ratio of absorbances at 1640 and 1545 cm^{-1}. For reasons of comparison, this figure also contains the ratio of the amide I (at 1650 cm^{-1}) to amide II (at 1545 cm^{-1}) amplitudes denoted by MF_1 and MF_2 for methods 1 and 2, respectively, and the scaling factor S versus time from method 2. The amplitudes of the bands used in both fit methods are given in Tables 3(a) and 3(b). It

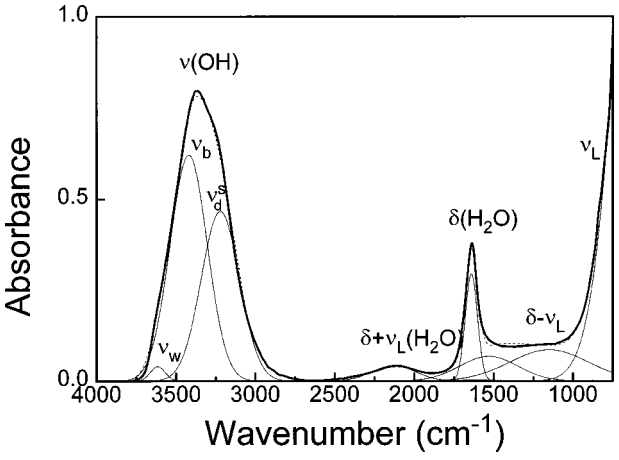

Fig. 2 Measured ATR-FTIR spectrum of water at room temperature (thick solid line) and spectral fit (dashed line) built up from individual vibrational bands (thin solid lines). Most important bands are the bending mode $\delta(H_2O)$ at 1640 cm^{-1}, the combination band $\delta+\nu_L$ at 2124 cm^{-1}, the symmetric ν_d^s(OH) stretch at 3225 cm^{-1}, the strong bond ν_b(OH) stretch at 3420 cm^{-1}, and the weak ν_w(OH) stretch at 3615 cm^{-1}.

Table 2 Fit parameters of the FTIR water spectrum given in Figure 2: band frequency (in cm^{-1}), bandwidth (in cm^{-1}), and amplitude (A in a.u.) and assignments after Scherer (Refs. 17 and 18). v=very; s=strong; m=medium; w=weak; br=broad; δ =deformation; ν=stretch.

Frequency (cm^{-1})	Bandwidth (cm^{-1})	Amplitude (a.u.)	Assignment
3615vw	65	0.040	ν_w(OH) weak bond stretch asymmetric di-H-bonded complex
3420 s	166	0.622	ν_b(OH) strong bond stretch asymmetric di-H-bonded complex
3220 s	171	0.466	ν_d^s(OH) stretch of symmetric di-H-bonded complex
2128 w	190	0.042	$\delta+\nu_L(H_2O)$ combination of 1640 and libration band
1640 s	54	0.294	$\delta(H_2O)$ bending
1520 m	258	0.067	combination band
1150 m	350	0.085	$\delta-\nu_L(H_2O)$ combination
487 s	264	2.362	ν_L libration band

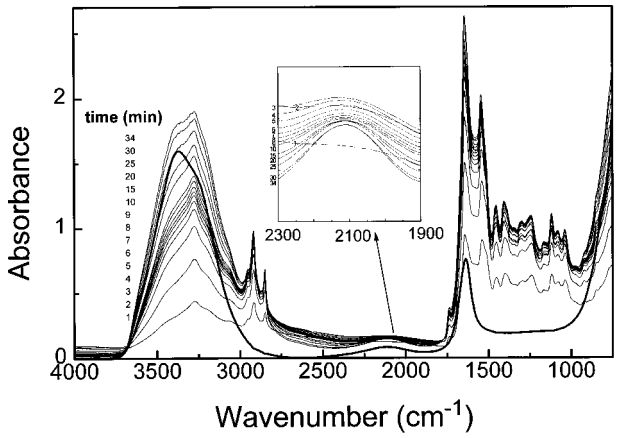

Fig. 3 Sequential hydrated human skin stratum corneum spectra measured during occlusion each minute for half an hour. The thick line represents the water spectrum (scaled twice) from Figure 2. Spectral changes can be clearly identified: increased contribution of the water bending mode at 1640 cm^{-1} and pronounced increase of the OH stretches in the high wave number band around 3300 cm^{-1}. Also the water combination band around 2125 cm^{-1} is clearly visible.

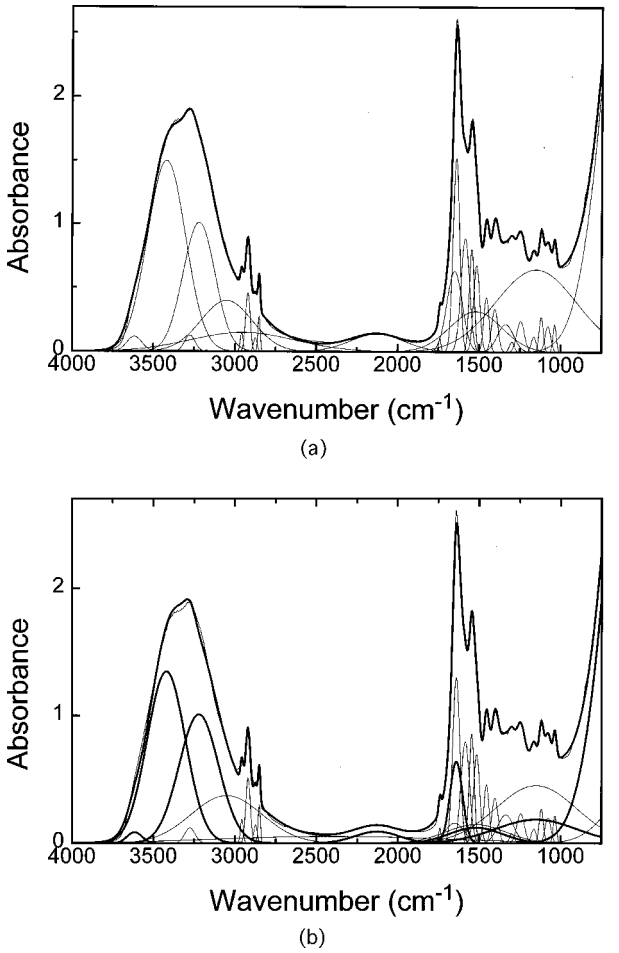

Fig. 4 Fits (thick line) to the ATR-FTIR spectra (upper thin line) of hydrated human stratum corneum: (a) using free water band amplitudes and band widths (fit method 1), and (b) using scaling factor S of the water spectrum as free parameter keeping ratios among individual water band amplitudes constant (fit method 2). Parameters in Table 3. In (b) the lower thick lines represent the individual water bands.

can be inferred from Figure 5 that the MF and the MF_1 slightly increase. The scaling factor S strongly increases from 0.3 to 2.1, while the MF_2 remains constant.

The amplitudes of the water bands from the free parameter fit (method 1) versus time are plotted in Figure 6. The amplitudes of the bending mode at 1640 cm^{-1} and the combination band at 2125 cm^{-1} are seen to ''saturate,'' while the OH stretch amplitudes continuously increase with time.

Error bars have been estimated from the band amplitudes. For example, in Figure 6, the relative error in the 1640 cm^{-1} band amplitude is less than 2% which can be inferred from the saturated part after 20 min. The relative error increases for lower signals, e.g., 5% for the 2125 cm^{-1} band. The sizes of the symbols in the figure are an indication of the errors.

4 DISCUSSION

4.1 HUMAN STRATUM CORNEUM SPECTRUM

The *in vivo* skin stratum corneum spectrum shown in Figure 1(a) best resembles that shown by Potts et al. (Fig. 1 in Ref. 7). On comparison with the *in vivo* spectrum by Wichrowski et al.[10] it is apparent that their spectrum contains a large double C=O peak at 1720 and 1740 cm^{-1}, a situation we only observed in spectra measured on the cheek and forehead (spectra not shown). The difference between *in vitro* and *in vivo* spectra is obvious from a comparison with the FTIR spectrum shown by Barry et al. (Fig. 2 in Ref. 25). The bands in the skin SC spectrum by Barry et al. are assigned on the basis of a comparison with *in vitro* FTIR and FT-Raman spectra. In our *in vivo* ATR-FTIR spectrum [see Figure 1(b)] we observe some bands in the lower wave number range that may correspond to some of the assignments of Raman bands which are not visible in their IR spectrum. For example, the 852 cm^{-1} δCCH band and the 883 cm^{-1} ρCH_2 band, the ν CC stretches at 1034 and 1118 cm^{-1}, and the 1168 cm^{-1} ν CC stretch, and δCOH bending. Some very weak bands indicated in the figure by their wave numbers are not assigned in the list of Barry et al., e.g., 917, 975, and 1337 cm^{-1}. Barry et al. assign two peaks at 1650 and 1656 cm^{-1} to α helix and disordered amide I νC=O stretches of the carbonyl groups of keratin proteins and ceramide lipids. We do not observe such a doublet. These bands are probably obscured by the strong band with a maximum absorbance at 1640 cm^{-1}. The weak shoulder at 1677 cm^{-1}, which becomes better visible in the

Table 3(a) Fit parameters (method 1) of the fits on hydrated stratum corneum spectra of Figure 3: band frequency (in cm^{-1}) and amplitude (in a.u.) vs time (min).

	Amplitudes (a.u.)														
	time (min)														
Frequency (cm^{-1})	1	2	3	4	5	6	7	8	9	10	15	20	25	30	34
3615	0.000	0.000	0.000	0.000	0.002	0.007	0.016	0.026	0.034	0.039	0.059	0.074	0.092	0.100	0.115
3420	0.118	0.300	0.502	0.620	0.682	0.735	0.780	0.836	0.891	0.935	1.102	1.197	1.317	1.424	1.497
3275	0.078	0.129	0.151	0.166	0.176	0.181	0.186	0.192	0.194	0.196	0.192	0.182	0.157	0.138	0.125
3220	0.114	0.234	0.356	0.419	0.449	0.476	0.499	0.534	0.572	0.603	0.717	0.781	0.873	0.954	1.009
3050	0.126	0.233	0.294	0.331	0.345	0.343	0.318	0.279	0.265	0.264	0.282	0.309	0.340	0.373	0.396
2957	0.044	0.088	0.116	0.131	0.141	0.147	0.152	0.156	0.159	0.162	0.168	0.167	0.161	0.154	0.146
2950	0.127	0.144	0.144	0.135	0.134	0.143	0.173	0.218	0.239	0.245	0.250	0.234	0.209	0.171	0.147
2919	0.187	0.320	0.388	0.427	0.452	0.466	0.478	0.489	0.497	0.503	0.517	0.515	0.496	0.478	0.460
2873	0.062	0.095	0.106	0.113	0.119	0.121	0.125	0.129	0.131	0.132	0.134	0.132	0.121	0.114	0.107
2850	0.127	0.206	0.240	0.261	0.275	0.283	0.291	0.299	0.304	0.307	0.316	0.314	0.300	0.290	0.280
2125	0.045	0.077	0.094	0.107	0.114	0.119	0.125	0.132	0.135	0.136	0.137	0.137	0.144	0.138	0.137
1740	0.019	0.050	0.072	0.085	0.094	0.101	0.106	0.112	0.115	0.117	0.126	0.128	0.125	0.120	0.110
1650	0.137	0.260	0.360	0.430	0.474	0.501	0.521	0.546	0.563	0.583	0.642	0.658	0.642	0.652	0.629
1640	0.549	0.862	1.056	1.162	1.219	1.252	1.284	1.307	1.339	1.366	1.448	1.482	1.484	1.499	1.519
1585	0.415	0.643	0.771	0.846	0.885	0.905	0.919	0.934	0.949	0.965	1.002	1.005	0.953	0.933	0.888
1545	0.303	0.491	0.610	0.685	0.733	0.760	0.782	0.802	0.821	0.837	0.881	0.892	0.857	0.837	0.807
1520	0.115	0.183	0.239	0.263	0.277	0.287	0.297	0.304	0.304	0.304	0.307	0.311	0.338	0.324	0.315
1515	0.488	0.708	0.794	0.844	0.869	0.877	0.882	0.887	0.893	0.897	0.889	0.859	0.767	0.722	0.678
1455	0.257	0.385	0.438	0.473	0.491	0.498	0.500	0.504	0.512	0.519	0.528	0.519	0.462	0.448	0.427
1403	0.202	0.304	0.349	0.379	0.394	0.401	0.405	0.409	0.415	0.420	0.426	0.417	0.375	0.357	0.335
1337	0.130	0.201	0.232	0.252	0.262	0.266	0.268	0.271	0.274	0.278	0.282	0.275	0.243	0.231	0.216
1298	0.016	0.036	0.051	0.060	0.066	0.070	0.074	0.077	0.079	0.080	0.086	0.087	0.086	0.083	0.080
1245	0.125	0.199	0.237	0.260	0.273	0.280	0.286	0.290	0.294	0.296	0.300	0.294	0.272	0.256	0.240
1164	0.010	0.042	0.065	0.081	0.092	0.099	0.105	0.110	0.114	0.118	0.129	0.133	0.129	0.126	0.121
1150	0.473	0.636	0.703	0.732	0.743	0.745	0.745	0.746	0.746	0.746	0.735	0.718	0.690	0.664	0.643
1118	0.123	0.193	0.237	0.263	0.279	0.287	0.295	0.301	0.306	0.311	0.319	0.319	0.307	0.293	0.274
1077	0.101	0.151	0.180	0.197	0.208	0.213	0.218	0.223	0.226	0.229	0.236	0.236	0.226	0.215	0.201
1035	0.148	0.205	0.234	0.249	0.258	0.262	0.265	0.268	0.270	0.271	0.270	0.264	0.249	0.234	0.217
489	1.615	2.376	2.969	3.287	3.448	3.566	3.658	3.757	3.878	3.989	4.433	4.709	5.068	5.399	5.620

Table 3(b) Fit parameters (method 2) of the fit on hydrated stratum corneum spectra of Figure 3: band frequency (in cm^{-1}), amplitude (in a.u.) vs time (min) and scaling factor *S*.

	Amplitudes (a.u.)														
	time (min)														
Frequency (cm^{-1})	1	2	3	4	5	6	7	8	9	10	15	20	25	30	34
4000	0.093	0.091	0.064	0.062	0.053	0.043	0.032	0.022	0.020	0.020	0.000	0.000	0.000	0.000	0.000
3275	0.073	0.148	0.177	0.168	0.167	0.187	0.200	0.214	0.211	0.201	0.172	0.169	0.144	0.132	0.119
3050	0.173	0.267	0.302	0.332	0.342	0.343	0.349	0.358	0.362	0.364	0.375	0.376	0.375	0.376	0.371
2957	0.051	0.089	0.121	0.157	0.177	0.176	0.177	0.177	0.183	0.192	0.214	0.211	0.207	0.198	0.190
2400	0.130	0.152	0.137	0.140	0.135	0.117	0.107	0.099	0.096	0.095	0.089	0.077	0.068	0.057	0.053
2919	0.197	0.326	0.400	0.462	0.499	0.503	0.510	0.515	0.525	0.538	0.570	0.564	0.548	0.528	0.513
2873	0.071	0.101	0.118	0.146	0.161	0.153	0.151	0.147	0.151	0.158	0.174	0.166	0.160	0.0150	0.145
2850	0.135	0.210	0.248	0.287	0.310	0.306	0.308	0.308	0.313	0.322	0.343	0.334	0.325	0.311	0.304
1740	0.018	0.046	0.066	0.079	0.089	0.094	0.097	0.099	0.101	0.104	0.114	0.117	0.119	0.119	0.120
1650	0.083	0.107	0.124	0.133	0.135	0.152	0.167	0.179	0.187	0.182	0.174	0.178	0.176	0.166	0.156
1640	0.507	0.836	1.037	1.117	1.182	1.228	1.262	1.288	1.304	1.326	1.380	1.398	1.350	1.327	1.299
1585	0.394	0.600	0.726	0.764	0.791	0.824	0.844	0.858	0.867	0.871	0.882	0.892	0.863	0.828	0.792
1545	0.304	0.501	0.636	0.708	0.756	0.791	0.817	0.840	0.859	0.875	0.919	0.935	0.913	0.890	0.860
1520	0.104	0.142	0.137	0.190	0.205	0.178	0.170	0.167	0.168	0.174	0.184	0.160	0.141	0.136	0.121
1515	0.481	0.700	0.804	0.827	0.846	0.874	0.892	0.901	0.905	0.901	0.877	0.858	0.803	0.741	0.695
1455	0.251	0.380	0.456	0.463	0.475	0.503	0.519	0.528	0.534	0.533	0.528	0.531	0.510	0.480	0.457
1403	0.198	0.300	0.359	0.372	0.385	0.403	0.415	0.423	0.427	0.428	0.425	0.423	0.402	0.375	0.352
1337	0.126	0.195	0.234	0.241	0.249	0.262	0.270	0.275	0.278	0.277	0.274	0.272	0.257	0.237	0.220
1298	0.016	0.035	0.048	0.059	0.065	0.067	0.069	0.072	0.074	0.076	0.082	0.082	0.079	0.077	0.073
1245	0.123	0.194	0.232	0.251	0.264	0.271	0.278	0.283	0.286	0.287	0.289	0.284	0.265	0.246	0.229
1164	0.008	0.038	0.061	0.075	0.085	0.092	0.098	0.104	0.107	0.110	0.120	0.124	0.121	0.117	0.111
1150	0.455	0.590	0.614	0.642	0.646	0.638	0.633	0.627	0.624	0.623	0.597	0.562	0.516	0.481	0.449
1118	0.122	0.191	0.235	0.260	0.276	0.283	0.291	0.297	0.302	0.306	0.315	0.315	0.301	0.287	0.268
1077	0.100	0.150	0.179	0.196	0.207	0.211	0.216	0.221	0.224	0.226	0.234	0.234	0.223	0.212	0.198
1035	0.148	0.205	0.234	0.250	0.258	0.261	0.264	0.267	0.269	0.270	0.270	0.264	0.248	0.232	0.215
489	0.918	1.127	1.118	0.938	0.881	0.983	1.039	1.079	1.040	0.973	0.771	0.778	0.657	0.591	0.527
S	0.299	0.534	0.783	1.001	1.093	1.099	1.112	1.134	1.204	1.282	1.554	1.671	1.873	2.045	2.166

derivative of the spectrum in Figure 1(b) has not been assigned. It could point to a partly β-sheet conformation of the amide I keratins.

4.2 WATER SPECTRUM

The simulation of the measured liquid water spectrum shown in Figure 2 has been achieved with as few as possible water bands. Acceptable fits were obtained without taking into account Fermi resonances between the overtone $2\nu_2$ and the νOH stretches, and without the asymmetric νOH stretch at 3440 cm^{-1}, which has been taken together with the 3422 cm^{-1} ν_bOH stretch band as one band. If more than three bands are used in the broad OH

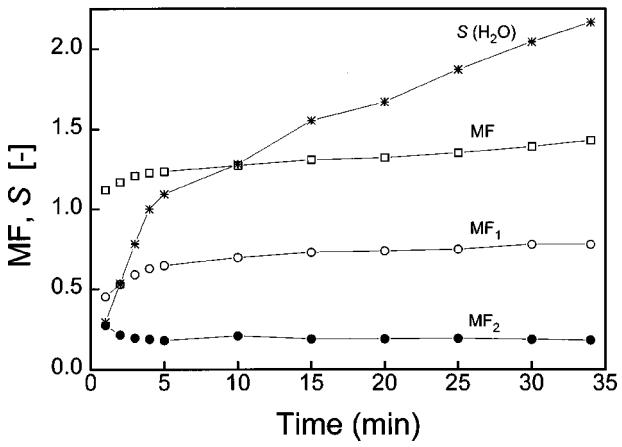

Fig. 5 Moisturing factor MF (squares) (ratio of absorbance at 1640 and 1545 cm^{-1}), amplitude ratio of amide I 1650 cm^{-1} to amide II 1545 cm^{-1} of fit methods 1 and 2 denoted by MF_1 (open circles) and MF_2 (solid circles), respectively, and scaling factor *S* (stars) vs time. Note that with fit method 2 the scaling factor *S* gradually increases with time representing the water content and MF_2 remains almost constant, while the MF and the MF_1 both slightly increase.

region it is always possible to obtain a better fit. Some imperfections in the fit are seen in the wings of the 1640 cm^{-1} bending band and around 2750 cm^{-1} where we lack some intensity. These may be due to the presence of another nearby water band or to an actual line shape different from a pure Gaussian.[27]

A Lorentzian component would give broader wings. Seshradi and Jones[27] state that the line shapes of infrared absorbance bands usually are a mixture of Lorentzian and Gaussian band shapes with a dominant Lorentzian contribution. In trying pure Lorentzians we found that it was impossible to get acceptable fits, especially in the high wave number wing of the 1640 cm^{-1} band, where the intensity is rather low. As shown, using pure Gaussians, the error between our measured spectrum and the fit is small and we therefore have chosen to continue using pure Gaussian band shapes, instead of introducing three more parameters per band.

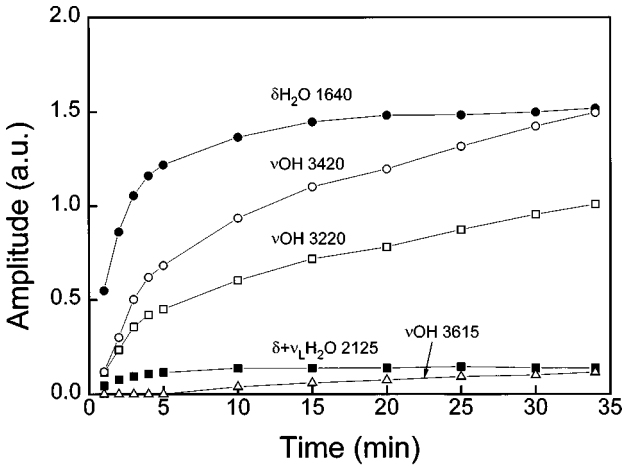

Fig. 6 Amplitudes of the water bands from the free parameter fit method 1 vs time. Note that the amplitudes of the bending mode at 1640 cm^{-1} and the combination band at 2125 cm^{-1} are seen to saturate, while the OH stretch amplitudes continuously increase with time.

The two broadbands at 1150 and 1520 cm^{-1} are necessary to fit the broad plateau between the libration band and the bending band. The assignments of these bands are not explicitly given by Scherer. Nonetheless, there are some possible combination bands that would add to this region.[28] For example the 1150 cm^{-1} band matches exactly the $\delta - \nu_L$ combination band. The $\nu_3 - \nu_2 - \nu_L$, $\nu_2 + \nu_3 - \nu_1$, and $\nu_1 - \nu_2 - \nu_L$ combination bands could possibly contribute to the other band. We did not find any information on the intensities of these combinations in the literature.

4.3 MONITORING HYDRATED SKIN STRATUM CORNEUM

The spectra in Figure 3 clearly show the increase in infrared signal intensity with time in the amide regions, and in the OH region. The thick line in Figure 3 representing the water spectrum (not drawn to scale) is included for comparison. Initially, the increase is due to the combined effect of water content increase and enhanced contact area between skin and the crystal. Hydration plastifies the upper keratine cells which makes it easier for the skin to conform to the crystal surface. After some time the contact area between skin and crystal reaches a maximum and the further increase in signal intensity is solely due to increased water content in the skin.

The spectral change in the combination band region around 2125 cm^{-1} is remarkable. At either side of this band the intensity *decreases* with time. Potts assumed the band area underneath the 1900 and 2300 cm^{-1} intensity line to be proportional to the contact area between skin and crystal. In our case, this area decreases. However, this cannot be due to a decreasing contact area. The spectral change in intensity is due to the combination of two effects: (1) increased contact area and (2) increasing contribution from absorption of water in the outermost layers of the skin SC, which in fact dilutes the skin SC spectrum with that of water. Absorbance *at either side* of the 2125 cm^{-1} band is low, therefore increased water content lowers the signal intensity in these regions.

One might wonder whether a changed penetration depth with water content would also add to the spectral changes observed. Hydration of the outermost skin layers affects the refractive index of these layers since the refractive index of dry SC is about 1.55 (Ref. 29) and that of water is about 1.33.[30] Therefore, hydration of skin SC continuously decreases the refractive index of skin SC.

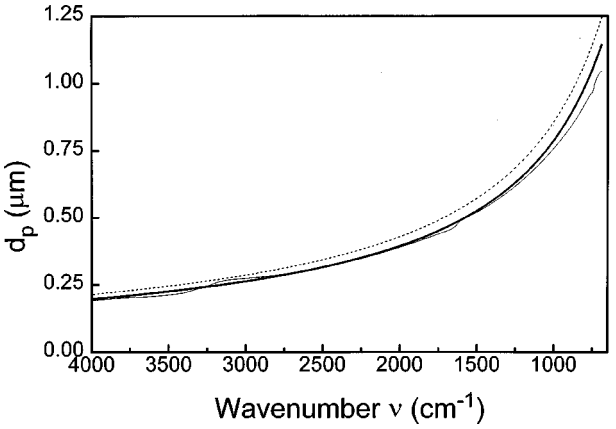

Fig. 7 Penetration depth of the IR beam as a function of the wave number according to Eq. (2) for ZnSe crystal $n_c = 2.42$. The thick solid line represents a sample with constant refractive index $n_s = 1.33$ (water), the thin solid line represents a sample with the actual wave number dependent refractive index of water $n_s(\nu)$, and the dashed line denotes a sample with refractive index $n_s = 1.55$ of dry stratum corneum. The actual refractive index spectrum of water was obtained from analysis of the measured water spectrum by the method described by Bertie et al. (Ref. 32).

4.4 PENETRATION DEPTH OF THE IR BEAM

The penetration depth d_p of the IR beam in the skin is given by[31]

$$d_p(\nu) = \left[2\pi\nu n_c \sqrt{\sin^2(\theta) - \left(\frac{n_s}{n_c}\right)^2} \right]^{-1}, \qquad (2)$$

with $\theta = 45°$ the angle of incidence, n_s the refractive index of the sample (skin), n_c the refractive index of the crystal ($n_c = 2.42$ for ZnSe), and $\nu = 1/\lambda$ the wave number and λ the wavelength in vacuum. At the penetration depth the evanescent field amplitude has dropped to $1/e$ of its original value. According to Eq. (2) the penetration depth is $d_p = 1.317\ \mu$m at $650\ \text{cm}^{-1}$ and $d_p = 0.214\ \mu$m at $4000\ \text{cm}^{-1}$ for dry SC (using $n_s = 1.55$), and $d_p = 1.21\ \mu$m at $650\ \text{cm}^{-1}$ and $d_p = 0.197\ \mu$m at $4000\ \text{cm}^{-1}$ for water ($n_s = 1.33$), see Figure 7. For the Ge crystal ($n_c = 4.0$) the penetration depths are about 50% lower than those for the ZnSe crystal. If fully hydrated skin SC would have a refractive index close to 1.33, the penetration depth would thus be only 8% less than the penetration depth in dry SC. The preceding calculation was based on a constant refractive index of water over the spectral range. We recalculated the penetration depth using Eq. (2) and the *actual* variation of the refractive index $n_s(\nu)$ of water across the water bands in the wave number range 4000–650 cm^{-1}. The refractive index of water $n_s(\nu)$ is obtained from our measured ATR-FTIR spectrum and analyzed by the transform method described by Bertie et al.[32] adapted for our system. The real and imaginary parts of the spectrum, which are directly coupled to the refractive index and absorption coefficient, are connected through the Kramers–Kronig relations. Taking the measured absorption spectrum of water as an initial guess for the absorption coefficient, iteratively calculating absorption coefficient and refractive index using the transform theory until the calculated absorbance spectrum fits the measured absorbance spectrum, the refractive index can be obtained. The result is that the penetration depth $d_p(\nu)$ at the 1640 and 3300 cm^{-1} bands, differs not more than 0.06 μm from that calculated with a constant refractive index of water ($n = 1.33$). It is therefore questionable whether the changed penetration depth of 8% adds to the observed spectral change around the 2125 cm^{-1} band.

We tried to find evidence for the presence of a thin layer of water between skin and crystal, which we expected to be formed during occlusion. A water film at the surface would show up in the spectrum immediately, especially in the OH stretch region and by diminished lipid band contributions. However, since the CH_2 and CH_3 bending bands of lipids do not disappear relative to the OH band we estimate that such a thin water film would probably be less than 0.1 or 0.05 times the penetration depth of about 0.2 μm around 3300 cm^{-1}, i.e., less than 20 nm thick.

4.5 FITS OF THE HYDRATED SKIN STRATUM CORNEUM SPECTRA

The fits on the spectra in Figure 4 have been obtained using as few bands as possible for the skin SC and water. Therefore, not all the bands in Table 1 are used in the fit, some minor important bands have been omitted. Some broadbands were required to match the background. In the fit of Figure 4(a) using free amplitudes (method 1) it is seen that two such bands at 2950 and 3050 cm^{-1} are used. The first band is underneath the symmetrical and asymmetrical CH_2, and CH_3 lipid stretch bands. The broad plateau is also present in the spectrum measured on the forehead skin SC which contains a rather large amount of sebum. The broadband might be attributed to a contribution of stretches of different CC chain lengths of the ceramides present in the SC. The 3050 cm^{-1} band has not been assigned in the list of Barry et al., it might be due to a CH stretch. The fit on the water spectrum of Figure 2 shows lack of intensity at the low wave number wing of the broad OH stretch region, which points to a possible contribution from another water band near this position.

The fit using the scaling factor S of the water spectrum (method 2) in Figure 4(b) also shows the need of two such broadbands. In the lower wave number spectral range an extra signal is needed at the position of the water bands. In the higher wave number range the OH bands are sufficient to fit the hydrated SC spectrum. This shows that the lower and higher wave number parts of the water spectrum do not proportionally contribute to the overall

hydrated SC spectrum. In other words, with increasing water content in the skin SC we observe a ''skewed'' growth of the actual water contribution to the skin SC spectrum.

This results from the variation in penetration depth over the wave number range. Since the signal in the lower wave number part of the spectrum is built up from deeper layers compared to the signal in the higher wave number region, the measured spectrum is a skewed representation of the contributions from different depths of the skin SC. A change in water content in a thin layer close to the skin SC surface would contribute relatively more to spectral changes in the higher wave number region since the penetration depth there is small (see Figure 7).

In fit method 2 using the scaled water spectrum, the fit is most sensitive to the change in OH stretches in the high wave number region, since these have the highest intensities, giving deviations between fit and measured spectra high weight.

4.5.1 Amplitudes in the Bending Mode Region and Moisturing Factor

In Figure 5 the MF as defined by Gloor, i.e., (Ref. 11) the ratio of the maximum absorbance at 1545 and 1640 cm^{-1}, and the MF_1 obtained from the amide I at 1650 cm^{-1} to amide II at 1545 cm^{-1} amplitude ratio from the free parameter fit (method 1) both increase gradually. The NH bending (amide II) band and C=O band (amide I) are sensitive to water by hydrogen bonding, as for example, is the case in hydration of hairs where the water molecules stack in between C=O and NH positions of the α-helical keratin backbone.[33] The apparent change in amplitudes of both amides however, is due to the combination of changed amide I and amide II bands and the increased water bending mode amplitude (and plateau).

The scaling factor S of method 2 increases from 0.3 to 2.1 while the MF_2 remains constant. Since the scaling factor is a contribution of the water spectrum with fixed interband amplitude ratios and since we have observed a skewed contribution when leaving the water band amplitudes free, S represents mainly the growth of the water bands with largest amplitudes (i.e., the OH bands). This means that in the bending mode region and the amides region the scaling factor is not directly comparable with the individual water band amplitudes and the observed constant MF_2 cannot be interpreted as being the independent contribution of water without affecting the amide I–II ratio. In Figure 4(b) this can be seen from the fact that besides the fixed water bands (lower thick lines) extra bands at 1150, 1550, and 1640 are needed to fit the spectrum.

The time behavior of the scaling factor S in Figure 5 follows more or less two linear parts. The first part (with slope of $dS/dt = 0.22$ units per minute) we address to an increase of water content and therefore also an increase in contact area. The second part (with slope $dS/dt = 0.037$ units per minute) is ascribed merely to the water content increase in the skin SC at maximum contact area.

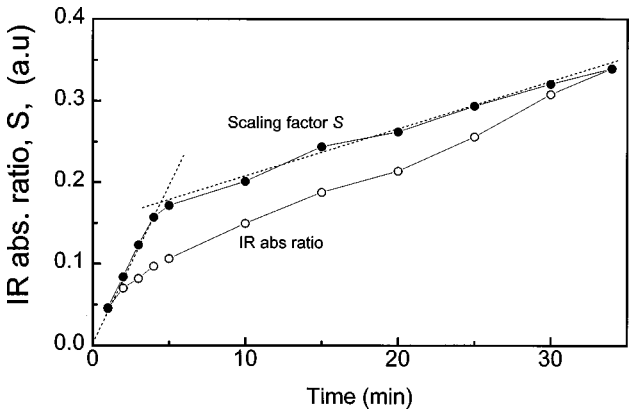

Fig. 8 IR absorbance ratio (open circles) and scaling factor S (solid circles) vs time. For comparison S has been scaled to match the IR absorbance ratio at time t is 34 min. The IR absorbance ratio is obtained from the ratio of the area under the measured spectra above and below the line connecting the 1900 and the 2300 cm^{-1} absorbance. Dashed lines indicate the almost linear regions of the signal increase due to the increased contact area between skin and crystal and increase of water content. It is seen that S exhibits a more distinct transition at the point of maximum contact area (crossing of the dashed lines). Also, S has a lower slope in the second increase traject, i.e., slower water content growth.

4.5.2 Water Band Amplitudes and Skewed Water Spectrum Contribution

From Figure 6 it can be seen that the amplitudes obtained from the free fit method of the water bending mode at 1640 cm^{-1} and the combination band at 2125 cm^{-1} saturate, while the OH band amplitudes continuously grow in time. The different growth of the water band amplitudes with time also means that the contribution from the water content increase is not homogenous over the spectrum. Following the discussion in Figure 4(b) this indicates that the actual water contribution to the SC spectrum is skewed, and is due to the contribution from different depths and the actual water concentration profile in skin SC depth.

4.5.3 Infrared Absorbance Ratio and the Scaling Factor S

In Figure 8 we compare the IR absorbance ratio method applied to our measured hydrated skin SC spectra in Figure 3 with the time dependence of the scaling factor S obtained from fit method 2. For the sake of comparison S has been scaled to match the IR absorbance ratio at time $t = 34$ min in the figure. It can be seen that the IR absorbance ratio and scaling factor S follow a similar pattern, although S exhibits a more distinct transition after the maximum contact area has been reached, and then approaches the IR absorbance ratio with a slightly lower slope.

The difference in slopes is due to the different approaches. The band shape of the combination band used in the Potts' method also changes by the effect of the wings of the neighboring bands of the 2125 cm^{-1} band. In our opinion the amplitudes fitted in the free fit method give a more direct representation of the water content increase.

4.5.4 Amplitudes in the OH Stretch Region

When comparing the ''free'' OH stretch amplitude time behavior in the higher wave number region with the ''fixed'' OH amplitudes scaled by the corresponding scaling factors *S*, in time it follows that the 3220 and 3615 cm^{-1} amplitudes closely match, while the scaled 3420 cm^{-1} amplitudes tend to be 10% lower than the free amplitudes. The minor difference is due to the somewhat different contributions from the two broadbands at 2950 and 3050 cm^{-1} in the free spectrum (method 1) and the 3050 cm^{-1} band in the fixed spectrum (method 2), respectively. The ratio of the weak to strong stretch band amplitudes is fairly constant after 5 min, indicating that in the time span measured here after reaching maximal contact area we find no significant change in the contributions of filling from strong H-bonded sites and weakly H-bonded sites in the SC.

4.5.5 NH Stretch Amplitude

The amplitude of the NH stretch at 3275 cm^{-1} exhibits a maximum in time as can be inferred from Tables 3(a) and 3(b). The first increase is again due to the increased contact area between skin and crystal. The decrease of the amplitude at a later time could be interpreted as the lower NH density by the influence of higher water content on the NH bonds through the filling of H bonds using the NH positions.

The fit analyses of the hydrated spectra have shown the separate contributions from water bands in the (hydrated) skin SC spectra. For determining the water content the free parameter fit method bears the advantage that the water bands (bending mode at 1640 cm^{-1}, combination band at 2125 cm^{-1} and the OH stretches) are varied individually and possible variations in, for example, strong and weak bond stretches can be obtained. However, in the time span of measurement in this study no significant variations in strong or weak bond stretch amplitudes have been observed.

Further details on separate contributions probably need longer (i.e., hours) hydration and corresponding monitoring. The second fit method shows the possibility to determine the water scaling factor *S* representing the contribution from the (fixed) water spectrum to the skin SC spectrum. The dependence of the scaling factor *S* or water content on time is shown to be comparable with that of Potts IR absorbance ratio applied to our data. Since we have used fixed amplitude ratios between the individual water bands in this fit, the scaling factor obtained here represents the fit factor of those water bands that are dominantly contributing to the hydration of the skin SC. In our case these are the OH stretch bands in the 3300 cm^{-1} region since these have the highest absorbance.

In our view, the fit method using the free bands gives the more realistic water contribution over the entire spectrum. The fit method using the scaling factor with fixed interband amplitudes shows the skewed water contribution depending on the penetration depth, and is realistic in the OH region.

As compared to the other three methods used, the fit analysis gives more insight in the changes due to contribution from the individual water bands and changes of the amide I and amide II bands. In the Potts method using the combination band region, we have shown that dilution of the skin SC spectrum by the increasing contribution of the water spectrum influences the absorbances at either side of the 2125 cm^{-1} combination band, especially at higher water content. The OH region is the most sensitive for changes in the outer SC cells because of the smaller penetration depth as compared to the low wave number region with deeper penetration. For an absolute measure of the water content a calibration is necessary as in the Potts method with similar measurements on *in vitro* dry skin SC.

5 CONCLUSIONS

Band fit analysis is used to quantitatively unravel water bands (bending mode at 1640 cm^{-1}, combination band at 2125 cm^{-1}, and three OH stretches) in hydrated skin SC ATR-FTIR spectra measured *in vivo*. Assignments of skin SC bands and of liquid water are given and compared with literature. The amplitudes found by the free parameter fit (method 1) determine the individual water content contributions. The bending band and combination band amplitudes are shown to saturate whereas the OH band amplitudes continuously increase with time, which results in a skewed ingrowth of the water spectrum in the skin SC spectrum.

A second fit method was used to determine the water scaling factor *S* representing the contribution of a water spectrum with fixed interband amplitude ratios into the skin SC spectrum. The time dependence of this scaling factor *S* is comparable to that of the IR absorbance ratio as used by Potts to determine water content. However, the scaling factor shows a more distinct transition from an increase in signal due to an enhanced contact area and that due to increased water content in the SC.

We think that fit analyses as shown here may help to further interpret water induced changes in skin SC spectra. In particular, we want to use the fit analysis to obtain changes in the water concentration profile[34] in skin depth, taking penetration depth over the spectral range into account. Similar

procedures could be useful in analyzing spectra of wool or hair.

Acknowledgments

The authors are indebted to the late Dr. H. E. Boddé for very stimulating discussions on the FTIR spectra and to Dr. G. J. Puppels for help and discussions on assignments of skin Raman and IR bands.

REFERENCES

1. R. O. Potts, ''Stratum corneum hydration: experimental techniques and interpretations of results,'' *J. Soc. Cosmet. Chem.* **37**, 9–33 (1986).
2. *Handbook of Non-Invasive Methods and the Skin*, J. Serup and G. B. E. Jemec, Eds., CRC Press, Boca Raton (1995).
3. N. A. Puttnam and B. H. Baxter, ''Spectroscopic studies of skin *in situ* by attenuated total reflectance,'' *J. Soc. Cosmet. Chem.* **18**, 469–472 (1967).
4. J. R. Hansen and W. Yellin, ''NMR and infrared spectroscopic studies of stratum corneum hydration,'' in *Water Structure at the Water Polymer Interface*, H. H. G. Jellinek, Ed., Plenum, New York, pp. 19–28 (1972).
5. R. L. Anderson, J. M. Cassidy, J. R. Hansen, and W. Yellin, ''Hydration of stratum corneum,'' *Biopolymers* **12**, 2789–2802 (1973).
6. K. Martin, ''Direct measurements of moisture in skin by NIR spectroscopy,'' *J. Soc. Cosmet. Chem.* **44**, 249–261 (1993).
7. R. O. Potts, D. B. Guzek, R. R. Harris, and J. E. McKie, ''A noninvasive, *in vivo* technique to quantitatively measure water concentration of the stratum corneum using attenuated total-reflectance infrared spectroscopy,'' *Arch. Dermatol. Res.* **277**, 489–495 (1985).
8. D. Bommannan, R. O. Potts, and R. H. Guy, ''Examination of stratum corneum barrier function *in vivo* by infrared spectroscopy,'' *J. Invest. Dermatol.* **95** (4), 403–408 (1990).
9. H. E. Boddé, L. A. R. M. Pechtold, M. T. A. Subnel, and F. H. N. de Haan, ''Monitoring *in vivo* skin hydration by liposomes using infrared spectroscopy in conjunction with tape stripping,'' in *Liposome Dermatics*, O. Braun-Falco, H. C. Korting, and H. I. Maibach, Eds., Springer-Verlag, Berlin, Heidelberg, pp. 137–149 (1992).
10. K. Wichrowski, G. Sore, and A. Khaïat, ''Use of infrared spectroscopy for *in vivo* measurement of the stratum corneum moisturization after application of cosmetic preparations,'' *Int. J. Cos. Sci.* **17**, 1–11 (1995).
11. M. Gloor, U. Wildebrandt, G. Thomer, and W. Kugerschmid, ''Water content of the horny layer and skin surface lipids,'' *Arch. Dermatol. Res.* **268**, 221–223 (1980).
12. D. A. Draegert, N. W. B. Stone, B. Curnutte, and D. Williams, ''Far-infrared spectrum of water,'' *J. Opt. Soc. Am.* **56** (1), 64–69 (1966).
13. D. Williams, ''Frequency assignments in infra-red spectrum of water,'' *Nature* **210**, 194–195 (1966).
14. Y. Marechal, ''Infrared spectra of water I, Effect of temperature and of H/D isotopic dilution,'' *J. Chem. Phys.* **95** (8), 5565–5573 (1991).
15. Y. Marechal, ''Infrared spectra of water II: Dynamics of H_2O (D_2O) molecules,'' *J. Phys. II France* **3**, 557–571 (1993).
16. Y. Marechal, ''Infrared spectra of a poorly known species: Water 3,'' *J. Phys. Chem.* **97**, 2846–2850 (1993).
17. J. R. Scherer, M. K. Go, and S. Kint, ''Raman spectra and structure of water in dimethyl sulfoxide,'' *J. Phys. Chem.* **77** (17), 2108–2117 (1973).
18. J. R. Scherer, M. K. Go, and S. Kint, ''Raman spectra and structure of water from −10 to 90°,'' *J. Phys. Chem.* **78**(13), 1304–1313 (1974).
19. M. Moskovits and K. H. Michaelian, ''A reinvestigation of the Raman spectrum of water,'' *J. Chem. Phys.* **69**(6), 2306–2311 (1978).
20. B. Curnutte and J. Bandekar, ''The intramolecular vibrations of the water molecule in the liquid state,'' *J. Mol. Spectrosc.* **41**, 500–511 (1972).
21. J. B. Bryan and B. Curnutte, ''A normal coordinate analysis based on the local structure of liquid water,'' *J. Mol. Spectrosc.* **41**, 512–533 (1972).
22. J. Bandekar and B. Curnutte, ''A local-structure model for calculation of lattice vibrations in liquid water,'' *J. Mol. Spectrosc.* **58**, 169–177 (1975).
23. W. A. P. Luck, ''Hydrogen bonds in liquid water,'' in *The Hydrogen Bond, Recent Developments in Theory and Experiments*, P. Schuster et al., Eds., North Holland, Amsterdam, pp. 1369–1420 (1976).
24. J. Israelachvili and H. Wennerström, ''Role of hydration and water structure in biological and colloidal interactions,'' *Nature* **379**, 219–225 (1996).
25. B. W. Barry, H. G. M. Edwards, and A. C. Williams, ''Fourier transform Raman and Infrared vibrational study of human skin: Assignments of spectral bands,'' *J. Raman Spectrosc.* **23**, 641–645 (1992).
26. H. G. M. Edwards, D. W. Farwell, A. C. Williams, B. W. Barry, and F. Rull, ''Novel spectroscopic deconvolution procedure for complex biological systems: vibrational components in the FT-Raman spectra of iceman and contemporary skin,'' *J. Chem. Soc. Faraday Trans.* **91**(12), 3883–3887 (1995).
27. K. S. Seshadri and R. N. Jones, ''The shapes and intensities of infrared absorption bands: A review,'' *Spectrochimica* **19**, 1013–1085 (1963).
28. G. Herzberg, ''Molecular spectra and molecular structure II,'' in *Infrared and Raman Spectra of Polyatomic Molecules*, Van Nostrand Reinhold, New York (1945).
29. P. T. Pugliese and A. J. Milligan, ''Ellipsometric measurement of skin refractive index *in vivo*,'' in *Bioengineering and the Skin*, R. Marks and P. A. Payne, Eds., MTP Press, Boston, pp. 291–302 (1981).
30. J. E. Bertie, M. K. Ahmed, and H. H. Eysel, ''Infrared intensities of liquids, 5. Optical dielectric constants, integrated intensities, and dipole moment derivatives of H_2O and D_2O at 22 °C,'' *J. Phys. Chem.* **93**, 2210–2218 (1989).
31. J. R. Reitz, F. J. Milford, and R. W. Christy, *Foundations of Electromagnetic Theory*, 3rd ed., Addison-Wesley, Reading, MA, p. 400 (1979).
32. J. E. Bertie and H. H. Eysel, ''Infrared intensities of liquids I: Determination of infrared optical and dielectric constants by FT-IR using the circle ATR cell,'' *Appl. Spectrosc.* **39**(3), 392–401 (1985).
33. C. Zviak, ''The science of hair care,'' in *Dermatology*, Vol. 7, Marcel Dekker, New York, p. 21 (1984).
34. S. L. Jacques, ''Water content and concentration profile in human stratum corneum,'' Dissertation, University of California, Berkeley (1984).